

Identification and Stability of the Nitrogenous Species in Zirconium Phosphate Oxynitride Catalysts

Nathalie Fripiat, Miguel-Angel Centeno,[†] and Paul Grange*

Laboratoire de catalyse et chimie des matériaux divisés, Université catholique de Louvain,
Place Croix du Sud 2/17 B-1348 Louvain-la-Neuve Belgium

Received July 10, 1998. Revised Manuscript Received November 27, 1998

A new family of basic phosphate oxynitride catalysts, ZrPON, has been synthesized by nitridation of high specific surface area zirconium phosphate precursor under ammonia flow. The identification study of the different nitrogenous species has been realized by the combination of XPS and DRIFTS analysis. The presence of NH_4^+ , NH_3 , $-\text{NH}_2$ and $-\text{NH}-$ groups has been evidenced on the solid surface while nitride N^{3-} anions replaced bulk oxygen O^{2-} species. The evolution of the concentration of the various species allows us to propose a mechanism for the nitridation of the precursor powder. The thermal stability of the ZrPON oxynitrides has also been studied by TPD-MS and DRIFTS. Nitrogen is removed from the ZrPON powder by a three-step desorption process depending on the temperature range considered. At low temperature ($<200^\circ\text{C}$), weakly physisorbed species are desorbed from the surface. In the $200\text{--}400^\circ\text{C}$ range, ammonia adsorbed on the Lewis acid sites is removed, and at higher temperature, terminal amino groups are attacked by gaseous water coming from hydroxyls condensation which results in the appearance of new hydroxyls bonded to phosphorus atoms.

1. Introduction

It is well-known that the incorporation of nitrogen in phosphate glasses, resulting in the formation of phosphorus–nitrogen bonds, improves their mechanical and chemical properties, i.e., strengthening of glass, increase of the glass-softening temperature, decrease of thermal expansion coefficient, and improvement of the aqueous durability.^{1–6} More recently, growing interest has been given to the use of non-oxide materials, in particular nitride and oxynitride powders, in heterogeneous catalysis as the different properties of these new materials compared to oxides or metals may lead to catalytic performances not attained with the latter. Indeed, the substitution of oxygen by nitrogen in the anionic network of high surface area oxide precursors gives rise to a new family of catalysts with original properties: the oxynitrides. One of the first researcher interested in this type of catalytic materials was Lednor, who started with the synthesis of SiO_xN_y .^{7,8} Several authors also related

the use of molybdenum, tungsten, and vanadium nitrides as efficient catalysts.^{9–18} Then the ALPON systems appear, largely described in the literature,^{19–26} and the other members of the family ZrPON,^{27–30} AlGa-

* Corresponding author. Telephone: (+32-10)473648. Fax: (+32-10)473649. E-mail: grange@cata.ucl.ac.be.

[†] On leave from Departamento de Química Inorgánica e Instituto de Ciencia de Materiales de Sevilla. Centro de Investigaciones Científicas Isla de la Cartuja. Universidad de Sevilla-CSIC. Sevilla. Spain.

(1) Leng-Ward, G.; Lewis, M. H. In *glasses and glass-ceramics*; Chapman and Hall: London, 1989.

(2) Brow, R. K.; Pantano, C. G. *Commun. Am. Ceram. Soc.* **1984**, C72.

(3) Larson, R. W.; Day, D. E. *J. Non Cryst. Solids* **1988**, 88, 97.

(4) Rocherulle, J.; Guyader, J.; Verdier, P.; Laurent, Y. *J. Mater. Sci.* **1989**, 24, 4525.

(5) Marchand, R.; Boukhir, L. *Ann. Chim. Fr.* **1985**, 10, 73.

(6) Hampshire, S.; Drew, R. A. L.; Jack, K. H. *Commun. Am. Ceram. Soc.* **1984**, C46.

(7) Lednor, P. W.; de Ruiter, R. *J. Chem. Soc., Chem. Commun.* **1991**, 1625.

(8) Lednor, P. W. *Catal. Today* **1992**, 15, 243.

(9) Oyama, S. T. *Catal. Today* **1992**, 15, 179.

(10) Hills, M. R.; Kemball, C.; Roberts, M. W. *Trans. Faraday Soc.* **1966**, 62, 3570.

(11) Aika, K.; Ozaki, A. *J. Catal.* **1969**, 14, 311.

(12) Choi, J. G.; Brenner, J. R.; Colling, C. W.; Demczyk, B. G.; Dunning, J. L.; Thompson, L. T. *Catal. Today* **1992**, 15, 201.

(13) Schlatter, J. C.; Oyama, S. T.; Metcalfe, J. E.; Lambert, J. M. *Ind. Eng. Chem. Res.* **1988**, 27, 1648.

(14) Volpe, L.; Boudart, M. *J. Sol. State Chem.* **1985**, 59, 332.

(15) Volpe, L.; Boudart, M. *J. Phys. Chem.* **1986**, 90, 4874.

(16) Wei, Z. B.; Xin, Q.; Grange, P.; Delmon, B. *J. Catal.* **1997**, 168, 176.

(17) Wei, Z. B.; Xin, Q.; Grange, P.; Delmon, B. *Solid State Ionics* **1997**, 101, 761.

(18) Kwon, H.-H.; Thompson, L. T. *Mater. Res. Soc.* **1996**, 454, 65.

(19) Conanec, R.; Marchand, R.; Laurent, Y. *High Temp. Chem. Processes* **1992**, 1, 157.

(20) Gandia, L. M.; Malm, R.; Marchand, R.; Conanec, R.; Laurent, Y.; Montes, M. *Appl. Catal. A* **1994**, 114, L1.

(21) Grange, P.; Bastians, Ph.; Conanec, R.; Marchand, R.; Laurent, Y. *Appl. Catal. A* **1994**, 114, L191.

(22) Grange, P.; Bastians, Ph.; Conanec, R.; Marchand, R.; Laurent, Y.; Gandia, L.; Montes, M.; Fernandez J.; Odriozola, J. A. In *Preparation of Catalysts VI*; Elsevier: Amsterdam, 1994; p 389.

(23) Benitez, J. J.; Odriozola, J. A.; Marchand, R.; Laurent, Y.; Grange, P. *J. Chem. Soc., Faraday Trans.* **1995**, 91, 4477.

(24) Massinon, A.; Odriozola, J. A.; Bastians, Ph.; Conanec, R.; Marchand, R.; Laurent, Y.; Grange, P. *Appl. Catal. A* **1996**, 137, 9.

(25) Massinon, A.; Conanec, R.; Marchand, R.; Laurent, Y.; Grange, P. *Stud. Surf. Sci. Catal.* **1996**, 101A, 77.

(26) Climent, M. J.; Corma, A.; Fornés, V.; Frau, A.; Guil-Lopez, R.; Iborra, S.; Primo, J. *J. Catal.* **1996**, 163, 392.

(27) Fripiat, N.; Grange, P. *J. Chem. Soc. Chem. Commun.* **1996**, 1409.

(28) Fripiat, N.; Conanec, R.; Auroux, A.; Laurent, Y.; Grange, P. *J. Catal.* **1997**, 167, 543.

(29) Fripiat, N.; Conanec, R.; Marchand, R.; Laurent, Y.; Grange, P. *J. Eur. Ceram. Soc.* **1997**, 17, 2011.

(30) Fripiat, N.; Grange, P. *J. Mater. Sci.*, submitted for publication.

PON,^{31–33} and VAION.^{34,35} This new family of catalysts has been successfully used in Knoevenagel condensation reactions.^{7,22,24,28,29} Some recent studies have also shown that they can be convenient supports for metal catalysts in dehydrogenation reactions.³¹

The O/N substitution is realized by a heat treatment of the precursor powder under ammonia flow. The main feature of these new materials lies in the control and adjustment of their acid–base properties during the nitridation step. The physicochemical characteristics of the synthesized oxynitrides have been studied, and their acid–base properties have been explored. From these studies, it has been shown that the basicity of all these solids is largely influenced by the nitrogen/oxygen ratio as an increase of both basic sites number and strength which is observed when the nitrogen content increases in the solid network.^{24,28,36}

The appearance of new basic centers in oxynitride solids may be then obviously associated with the presence of nitrogen atoms in the initial oxide structure. Indeed, the reactivity of ammonia with the oxide precursor powder involves the presence of various nitrogenous species in oxynitride solids.

The first reactions to be considered are acid–base interactions. Indeed, ammonia can act as a base and first react with Brønsted or Lewis acid sites. In the first case, the ammonia adsorption on terminal metal–OH species of the oxide will result in the formation of O^-NH_4^+ ammonium ions while coordinatively bonded NH_3 will be formed by adsorption on Lewis acid sites. In phosphate glasses, further nitridation allows nitrogen from ammonia to replace either bridging or nonbridging oxygen in the precursor network to produce nitride N^{3-} anions.^{37–39} This last nitrogen species is supposed to be the most abundant in phosphate oxynitride glasses and two bonding states are identified, depending on the N coordination. Nitrogen could be linked with three single bonds to phosphorus atoms as tricoordinated nitrogen



or nitrogen could be bonded to phosphorus by one single and one double bond as bicoordinated nitrogen $\text{P}=\text{N}-\text{P}$. Some hydrogenated nitrogen atoms can also be found at the solid surface and in this case, amine groups, metal– NH_2 , or imide groups, metal– NH –metal, are formed by ammonia substitution of surface hydroxyl groups. Finally, although this reaction is quite improbable, the replacement of phosphorus atoms by

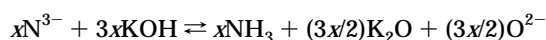
nitrogen of ammonia could also be envisaged, resulting in the formation of nitrate NO_3^- functions.

The aim of this work is to investigate the various nitrogen species responsible for the enhancement of the basicity in the ZrPON system and to study their stability. Spectroscopic methods as XPS (X-ray photoelectron spectroscopy) and DRIFT (Diffuse reflectance infrared spectroscopy) have been used as well as temperature-programmed treatments coupled to a mass spectrometer.

2. Experimental Section

Materials. The citrate method was used to prepare the high surface area amorphous phosphate precursor.²⁹ A 20 g of $\text{ZrO}(\text{NO}_3)_2 \cdot 3.4\text{H}_2\text{O}$ (Acros Chimica, 99.5%) was dissolved by light heating in 250 mL of distilled water. Then 20 mL of a 0.37 M (H_3PO_4) (Fluka) solution was then added. The Zr/P atomic ratio was fixed at 0.9. After the mixture was stirred for 1 h, an excess of citric acid (Merck, p.a., 55 g) was added to the viscous and gelatinous precipitate. The resulting product was further stirred overnight. Water was then evaporated under reduced pressure, and the precipitate was dried for 20 h at 120 °C under vacuum (50 mbar). The sample was then calcined for 16 h at 500 °C. An amorphous zirconium phosphate (ZrPO) precursor with high specific surface area (230 m^2/g) is obtained. Nitridation of the phosphate precursor was carried out under flowing pure ammonia. Various nitrogen contents were obtained by modification of both nitridation time and temperature within the ranges 0.75–73 h and 590–790 °C, respectively. At the end of the activation process, the samples were allowed to cool to room temperature under a pure and dry nitrogen flow. The ZrPON oxynitrides are still amorphous and their specific surface area ranges from 115 m^2/g for the more nitrided samples to 210 m^2/g for the less nitrided samples.

Two chemical methods were used to establish the nitrogen content of the samples. (i) The total nitrogen content was determined by displacement reaction of nitride ions N^{3-} induced by an excess of strong molten base at 400 °C which leads to the formation of ammonia



according to a previously described procedure.⁴⁰ The ammonia was then dissolved in water and titrated with a sulfuric acid solution. The accuracy of this determination is ~10% while the reproducibility is estimated at ~5%. (ii) Surface nitrogen (NH_x species) concentration was measured by a Kjeldahl type method: The ZrPON sample (75 mg) was suspended in 10 mL of saturated KOH solution to which 30 mL of distilled water was added. The liberated ammonia was then carried out to a receiving flask by steam distillation, condensed, and collected in an acid boric solution (10 g/L) with a mixed methylene blue–methyl red indicator. This solution was titrated by 0.01 N sulfuric acid.

Instruments. An ESCA spectrometer (model SSX100, Surface Science Laboratories) was used to analyze the surface compositions up to 50 Å of the samples. The SSX100 instrument is interfaced with a Hewlett-Packard 9000/310 computer allowing instrument control, data accumulation, and processing and equipped with a monochromatized $\text{Al(K}\alpha)$ X-ray source (1486 ± 1 eV). A low energy electron flood gun (set at 6 eV) with a Ni grid placed 3 mm above the samples was used to control charging on nonconductive sample surfaces. The sample powders were pressed in small stainless steel troughs of 4 mm diameter and introduced in the spectrometer at room temperature. Then, they were degassed at 120 °C in the preparation chamber (10^{-7} Torr). During the analysis, the pressure in the analysis chamber was around 10^{-9} Torr. The

(31) Guéguen, E.; Delsarte, S.; Peltier, V.; Conanec, R.; Marchand, R.; Laurent, Y.; Grange, P. *J. Eur. Ceram. Soc.* **1997**, *17*, 2007.

(32) Peltier, V.; Conanec, R.; Marchand, R.; Laurent, Y.; Delsarte, S.; Guéguen, E.; Grange, P. *Mater. Sci. Eng.* **1997**, *B47*, 177.

(33) Delsarte, S.; Peltier, V.; Laurent, Y.; Grange, P. *J. Eur. Ceram. Soc.* **1998**, *18*, 1287.

(34) Wiame, H.; Bois, L.; L'Haridon, P.; Laurent, Y.; Grange, P., *J. Eur. Ceram. Soc.* **1997**, *17*, 2017.

(35) Wiame, H.; Bois, L.; L'Haridon, P.; Laurent, Y.; Grange, P. *Solid State Ionics* **1997**, *101–103*, 755.

(36) Baraton, M. I.; Chen, X.; Gonsalves, K. E. *Mater. Res. Soc.* **1996**, *454*, 59.

(37) Bunker, B. C.; Tallant, D. R.; Balfe, C. A.; Kirkpatrick, R. J.; Turner, G. L.; Reidmeyer, M. R. *J. Am. Ceram. Soc.* **1987**, *70*, 675.

(38) Day, D. E. *J. Non-Cryst. Solids* **1989**, *112*, 7.

(39) Marchand, R.; Agliz, D.; Boukbir, L.; Quemerais, A. *J. Non-Cryst. Solids* **1988**, *103*, 35.

(40) Guyader, J.; Grekov, F. F.; Marchand, R.; Lang, J. *Rev. Chim. Miner.* **1978**, *15*, 341.

irradiated zone was an elliptical spot, with a shorter axis of 1 mm. The constant pass energy in the hemispherical analyzer was 50 eV. For each sample, a wide scan (0–1000 eV binding energy) was performed, followed by a detailed scan of C_{1s} , Zr_{3d} , P_{2p} , O_{1s} , N_{1s} , and finally C_{1s} again to check for the absence of sample degradation. The binding energy (E_b) of the main lines was determined by setting the value of 284.8 eV for the C_{1s} component due to carbon only bound to carbon and hydrogen. The peak area was determined with Shirley type nonlinear background subtraction.⁴¹ The spectra were decomposed with the least-squares fitting routine provided by the manufacturer with a Gaussian/Lorentzian ratio of 85/15. The atomic ratios were calculated from relative intensities corrected by the elemental sensitivity factors provided by the manufacturer (C_{1s} , 1.00; Zr_{3d} , 7.47; P_{2p} , 1.30; O_{1s} , 2.49; N_{1s} , 1.68) (mean free path varying according to the 0.7th power of the photoelectron kinetic energy; Scofield cross-sections;⁴² transmission function assumed to be constant). The relative uncertainty of element concentration measurements is estimated at 10%, while the absolute uncertainty on binding energy determination is estimated at ± 0.2 eV.

Diffuse reflectance infrared Fourier transform spectroscopy (DRIFTS) spectra were collected from a controlled environmental chamber (Spectra Tech 0030-103) equipped with ZnSe windows. The chamber, which allows in situ temperature treatment up to 900 °C under controlled atmosphere, is mounted in a Brüker IFS 88b FTIR spectrometer with KBr optics and a DTGS detector operating at 4 cm^{-1} resolution. Samples were placed inside the chamber without any treatment such as pressure or dilution. Then they were heated in situ under a 30 mL/min N_2 flow. A total of 200 scans were accumulated at different temperatures, after 1 h of heating at the indicated temperature. An aluminum mirror is used as background, and data are presented in absorbance mode without any treatment.

Temperature programmed treatments were performed in a conventional flow apparatus using a U tube quartz reactor connected on line with a quadrupole mass spectrometer (modified GCD from HP) for continuous analysis of the gas effluents. Mass spectra were recorded in scan mode on the range of 10 to 200 amu. The temperature programmed pretreatment (TPP) tests were carried out in a pure He flow (50 mL/min) from room temperature to 800 °C (rate of 10 °C/min). The identification of various species desorbed during the thermal process was done by re-analyzing the total ion spectra for the specific mass. The main desorbed species detected are water, ammonia, dinitrogen, and carbon dioxide for which the evolution of $m/e = 18$, $m/e = 17$, $m/e = 28$, and $m/e = 44$ respectively have been followed. The reason the $m/e = 17$ rather than $m/e = 16$ used usually for ammonia have been chosen is the possibility of the appearance of oxygenated molecules which can take part in $m/e = 16$ fragmentation. The $m/e = 17$ is preferred, though this signal also includes a water fragmentation participation. But it is possible to calculate the relative abundance of $m/e = 17$ only due to ammonia as the relative water fragmentation ratio of abundance $m/e = 17$ /abundance $m/e = 18$ is given by the constructor as equal to 21.22%. Ammonia released during this pretreatment was collected and trapped in a boric acid solution (10 g/L) and then titrated by 0.01 N sulfuric acid for quantitative determination.

The specific surface area was measured by the single point BET method ($p/p_0 = 0.3$) in a Micromeritics Flowsorb 2000 apparatus. Samples were degassed for 1 h at 150 °C under nitrogen flow before analysis at liquid nitrogen temperature.

3. Results and Discussion

3.1. Identification of Nitrogen Species. *a. Experimental Results.* As described in the Experimental Section, two chemical techniques were used for the quan-

Table 1. Total and Kjeldahl Nitrogen Content of the ZrPON Series

samples	nitridation		tot. N determ		surf. N determ	
	time (h)	T (°C)	N_T (wt %)	after 2 years	N_K (wt %)	after 2 years
ZrPON1	0.75	590	1.8	0.8	0.5	0.4
ZrPON2	0.50	790	5.4	5.1	0.3	0.3
ZrPON3	12.75	700	8.2	7.8	0.9	0.6
ZrPON4	14.25	750	11.2	10.6	0.8	0.8
ZrPON5	73	790	19.0	17.2	4.2	3.2

titative determination of nitrogen content in zirconophosphate oxynitrides. The first one allows to measure the total nitrogen amount (N_T) which consists of nitride anions in bulk solids (N^{3-}) as well as NH_x ($1 = x = 4$) surface species. The second method only gives access to the NH_x species denominated N_K for the Kjeldahl principle on which it is based.

As observed in Table 1 (columns 4 and 6), all the values of N_T are larger than their equivalent N_K which is not surprising since N_T determination included N_K values. It can also be pointed that N_K content is quite negligible (< 1 wt %) regardless to total nitrogen amount except for the more nitrated sample (ZrPON5).

The chemical determinations described above allow the quantification of nitrogen but they do not give any information about qualitative identification. XPS analyses were performed in order to obtain these data. The XPS spectrum of N_{1s} electrons can be decomposed into 2 Gaussian curves (fwhm of 2.00 and 1.75 eV) (Figure 1), except for the less nitrated sample for which three peaks are observed. These overlapping peaks are indicative of nitrogen present in more than one chemical form. The assignation of the different signals will be detailed in a further paragraph. The binding energy of the more energetic component has been fixed to 399.2 eV while the second peak is located around 397.7 eV. The binding energy of this last signal decreases by 0.6 eV when N_T increases from 0 to 19 wt % in the bulk phase (Figure 2). An additional peak at 400.4 eV is observed for the less nitrated samples (1.8 wt % N). Nitrate species are not present in oxynitrides samples as no peak is detected over 402 eV. Figure 3 shows the evolution of the two main nitrogen species concentration as total N content increases in the solids. The relative values were deduced from the respective areas of these two species. The evolution of the total area of the nitrogen signal is also plotted. The nitrogen to oxygen substitution involves simultaneously the evolution of the two types of nitrogen atoms: the peak analyzed at higher energy, predominant in the less nitrated sample, reaches quickly a limiting value close to 3.5 at. % while the intensity of the second N_{1s} component increases sharply with the total nitrogen content. At low N content, the surface and bulk nitrogen concentration are identical. Indeed, the diagonal dotted line in Figure 3 is representative of equivalent N concentrations at the surface and in the bulk. As seen from this figure, the total XPS nitrogen concentration in the two first nitrated samples is located on the diagonal. However, when the total nitrogen concentration of the solid increases further, the surface nitrogen concentration increases more slowly. This could be attributed to an oxidation of the surface due to water adsorption and therefore the relative concentration of surface oxygen atoms increases while

(41) Shirley, D. A. *Phys. Rev.* **1972**, B5, 4709.

(42) Scofield, J. H. *J. Electron Spectrosc. Relat. Phenom.* **1976**, 81, 129.

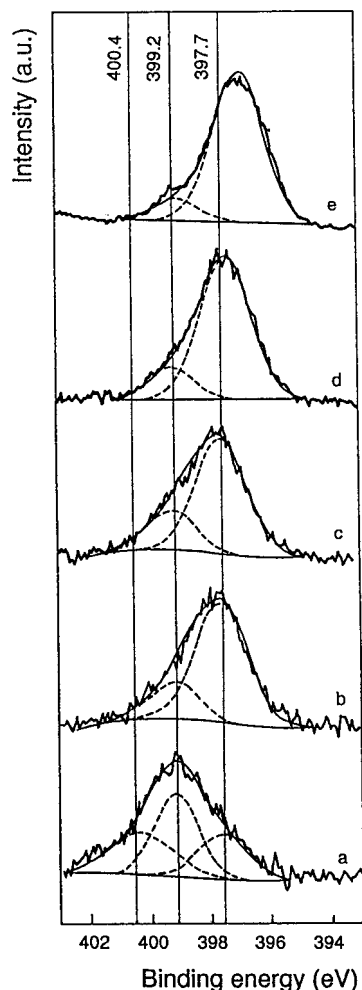


Figure 1. N_{1s} XPS spectra of ZrPON samples at (a) 1.8, (b) 5.4, (c) 8.2, (d) 11.2, and (e) 19 wt %. The relative intensities of each spectrum have been normalized.

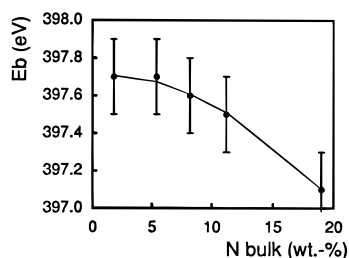


Figure 2. Evolution of the binding energy of nitride anions N_{1s} electrons with the total N content.

the concentration of the other surface atoms decreases. Some systematic errors associated with the manufacturer's sensitivity factors might also account for differences observed between XPS and bulk nitrogen content.

Infrared spectroscopy gives additional information about the nitrogenous species. DRIFT spectra of ZrPON1 (1.8 wt % N) heated under a pure N_2 flow at different temperatures, as shown in Figure 4, illustrate the hypothesis proposed above. At room temperature, whatever the N content, the spectrum is dominated by a large band centered around 3300 cm^{-1} which is assigned to hydrogen-bridged bonds (OH) and NH stretching. The increase of the temperature induces the departure of adsorbed water, and then, better defined peaks appear at 3740 and 3660 cm^{-1} . They are at-

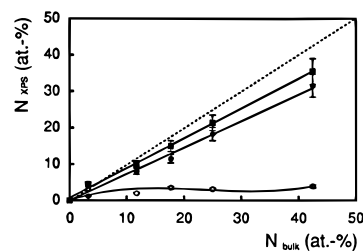


Figure 3. Evolution of XPS nitrogen concentration (■) total, (●) nitride anions N^{3-} , and (○) NH_x species as a function of total nitrogen content N_T determined by chemical analysis (both expressed in atomic percentage).

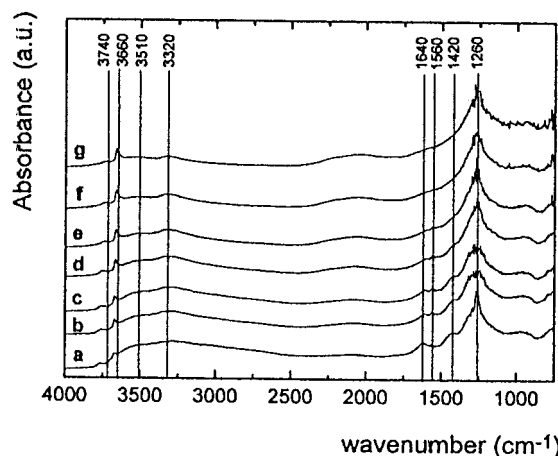


Figure 4. DRIFT spectra of ZrPON1 (1.8 wt % N) (a) at room temperature and heated at (b) 100, (c) 200, (d) 300, (e) 400, (f) 500, and (g) 600 °C.

tributed to the vibrational modes of hydroxyl groups linked to metal atoms: ν_{Zr-OH} and ν_{P-OH} respectively.^{43,44} However, a large band due to a stretching mode of NH_x species remains centered around 3320 cm^{-1} .⁴⁵ Climent et al.²⁶ have succeeded in the identification of various NH_x species in AIPON solids by decomposition of this last band into three components. They have identified ν_{N-H} in (i) $Me-NH_2$ at 3480 cm^{-1} with $Me = Al$ or P , (ii) $Me-NH_2$ and mainly $Me-NH-Me$ at 3370 cm^{-1} , and (iii) adsorbed NH_3 and/or NH_4^+ at 3300 cm^{-1} . When a zoom is performed on the $3000\text{--}4000\text{ cm}^{-1}$ spectral area of ZrPON1 (Figure 5), two weak shoulders superimposed to the main signal may be observed at 3400 and 3270 cm^{-1} . By comparison with the AIPON infrared spectra obtained by Climent et al., these signals may be assigned to NH vibrations in $Me-NH_2$ (3400 cm^{-1}) ($Me = Zr$ or P), $Me-NH_2/Me_2-NH$ vibrations (3320 cm^{-1}) and NH_3/NH_4^+ (3270 cm^{-1}). The energy shift observed with AIPON solids can be explained by the presence of zirconium atoms instead of aluminum. Other interesting vibrations are observed at lower energy. The main band located at 1260 cm^{-1} is due to the combination of asymmetric $P-O$, $P=O$, or $P-N$ stretching modes ν_3 in PO_4 tetrahedra.²³ This band becomes larger and larger with the temperature of the treatment and its frequency decreases linearly from 1260 to 1190 cm^{-1} with N_T as illustrated in Figure 6 representing the DRIFT spectra of the different ZrPON

(43) Yamaguchi, T. *Bull. Chem. Soc. Jpn.* **1978**, *51*, 2482.

(44) Rebenstorf, B.; Lindblad, T.; Andersson, L. T. *J. Catal.* **1991**, *128*, 293.

(45) Moffat, J. B. *Catal. Rev. Sci. Eng.* **1978**, *18*, 199.

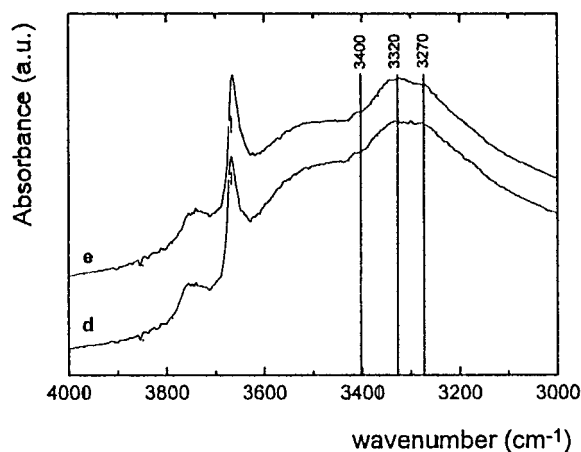


Figure 5. Zoom performed in the 3000–4000 cm^{-1} energy range of spectra e and d presented in Figure 4.

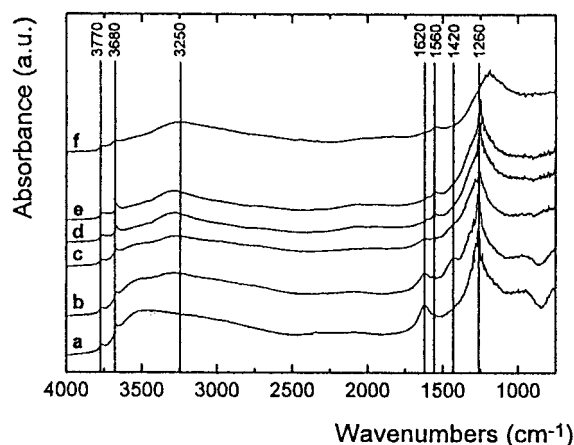


Figure 6. DRIFT spectra of ZrPON solids heated for 1 h at 100 °C: (a) 0, (b) 1.8, (c) 5.4, (d) 8.2, (e) 11.2, and (f) 19 wt % N.

solids heated in situ for 1 h at 100 °C. The peaks around 1400–1600 cm^{-1} correspond to various N–H_x vibrations. The signal at 1420 cm^{-1} is due to the asymmetric bending deformation $\delta_{\text{N-H}}$ mode of surface NH_4^+ ions. The band at 1560 cm^{-1} is characteristic of the presence of terminal amino groups bonded to the metal atoms (P or Zr) Me-NH_2 . This peak has already been described for other metal oxides, i.e., AlPON ,²³ SiO_xN_y ,⁴⁶ and AlN .⁴⁷ Finally the band at 1640 cm^{-1} is attributed to both physisorbed water and/or ammonia adsorbed on Lewis acid sites which are proved to be present on ZrPON surface.²⁸ As observed on Figure 4, the bands located at 1640 and 1420 cm^{-1} decrease upon temperature. At 400 °C, only the Me-NH_2 vibration remains while NH_4^+ cations and ammonia molecules are totally desorbed from the ZrPON surface. As seen from Figure 6, the nitrogen content is higher in the ZrPON solids, the NH_4^+ and $\text{NH}_3/\text{H}_2\text{O}$ bands area, is lower and the intensity of vibrations due to Me-NH_2 (1560 cm^{-1}) and NH_x species is higher (3300 cm^{-1}).

b. Discussion. • Identification of Nitrogen Species in Zirconium Phosphate Oxynitrides. From the results described above, it seems clear that the nitrogen species can be classified in two categories. The first one consists

Table 2. N_{1s} Binding Energy Attribution from the Literature of Some Nitrided Compounds^a

Compound Type	N1s Binding Energy (eV)						
	396	397	398	399	400	401	402
<div>nitride anion N³⁻</div>							
→ Nitride samples ³⁸							
→ Metallic nitrides ^{47,48,51,60,61}							
→ Phosphate glasses ^{39,54,56,61}							
<div>$\begin{array}{c} \text{P}=\text{N}-\text{P} \\ \\ \text{P} \\ \\ \text{N}-\text{P} \\ \\ \text{P} \end{array}$</div>							
→ P ₃ N ₅ H ₁₃ ⁵³							
→ P ₃ N ₅ ^{52,53}							
<div>amino NH₂ and imido NH groups</div>							
→ AlN ⁴⁷ , Si ₃ N ₄ ⁵¹ , BON ⁶⁰							
→ Phosphate glasses ^{52,54,56,61}							
<div>$\begin{array}{c} -\text{N}- \\ \\ -\text{NH}_2 \end{array}$</div>							
<div>ammonia NH₃</div>							
→ liquid ³⁸							
→ adsorbed ^{47,52}							
<div>ammonium cations NH₄⁺^{52,58,60}</div>							
<div>nitrate⁵⁸</div>							

^a The shaded regions are representative of N_{1s} experimental binding energy ranges in ZrPON oxynitride spectra.

of the N^{3-} nitride anions, which are introduced in the ZrPON structure in exchange for the oxygen atoms of the bulk during the nitridation process in the ratio of three oxygens for two nitrogens. The second class counts several hydrogenated nitrogen molecules located at the ZrPON surface. They are called “ NH_x ” species with $1 \leq x \leq 4$.

An accurate identification of nitrogenous species is made possible by comparison with data given in the literature. Table 2 shows the N_{1s} XPS binding energy attribution of various nitrided samples described by different authors. The three shaded vertical bands correspond to the different N_{1s} binding energy values observed for ZrPON described in this study. The N_{1s} XPS signal is much debated but, generally, the energy range for nitride anions N^{3-} in nitride samples, as for example ZrN ,^{48–50} AlN ,⁴⁷ Si_3N_4 ,⁵¹ VN ,⁵² or P_3N_5 ,^{52,53} is varied from 396.2 to 398.5 eV (Table 2). However, in metaphosphate oxynitride glasses,^{38,39,54,55} two kinds of nitride anions (N^{3-}) are identified depending on whether

(48) Milosev, I.; Strehblow, H. H.; Gaberscek, M.; Navinsek, B. *Surf. Interface Anal.* **1996**, 24, 448.

(49) Prieto, P.; Galan, L.; Sanz, J. M. *Surf. Interface Anal.* **1994**, 21, 395.

(50) Prieto, P.; Galan, L.; Sanz, J. M. *Phys. Rev.* **1993**, B47, 1613.

(51) Kubler, L.; Haug, R.; Koulmann, J.-J.; Belmont, D.; Hill, K.; Jaegle, A. *J. Non-Cryst. Solids* **1985**, 77–78, 945.

(52) Hendrickson, D. N.; Hollander, J. M.; Jolly, W. L. *Inorg. Chem.* **1969**, 8, 2643.

(53) Veprek, S.; Iqbal, Z.; Brunner, J.; Schärli, M. *Philos. Mag.* **1981**, 43, 527.

(54) Brow, R. K.; Reidmeyer, M. R.; Day, D. E. *J. Non-Cryst. Solids* **1988**, 99, 178.

(55) Marchand, R.; Laurent, Y.; Quémerais, A. *Riv. Stn. Sper.* **1990**, 5, 101.

(46) Lednor, P. W.; De Ruiter, R.; Emeis, K. A. *Mater. Res. Soc. Symp. Proc.* **1992**, 271, 801.

(47) Liu, H.; Bertolet, D. C.; Rogers, J. W. *Surf. Sci.* **1995**, 340, 88.

they are bonded to three phosphorus atoms by three single bonds (tricoordinated $>\text{N}-$) or to two phosphorus atoms by one double bond and one single bond (bicoordinated $=\text{N}-$). A triple bonding $\text{N}\equiv$ is inconsistent with the tetrahedral environment of phosphorus atoms in such compounds. The peak at lower energy (397.8 eV) is assigned to bicoordinated atoms while the larger values (399.3 eV) are attributed to tricoordinated atoms (Table 2). Generally the authors excluded the presence of $\text{N}-\text{H}$ bonds in metaphosphate glasses so these assignments concern only the nitride anions N^{3-} . However, Brow et al.⁵⁶ have studied the properties and the structure of $\text{P}-\text{O}-\text{N}-\text{H}$ glasses and they suggest the decomposition of N_{1s} XPS spectra of such glasses into three Gaussian curves: the first one, located around 398 eV, has been attributed to bicoordinated nitride nitrogen while the second peak, around 399.8 eV, has not been assigned to tricoordinated nitride nitrogen species as in bulk nitrated metaphosphate glasses but to imidophosphate species ($\text{P}-\text{NH}-\text{P}$). Finally the third one, situated around 402 eV, is due to diprotonated amino nitrogen ($\text{P}-\text{NH}_2$). These authors also underline that these assignments are consistent with those made for N_{1s} spectra collected from the surface of some other nitrated samples. In the case of SiN_xH_y films for example, $\text{Si}-\text{NH}-\text{Si}$ has a binding energy around 399 eV, while the nitride peak is located at 397.7 eV.^{51,57} Some other data concerning the attribution of NH_x nitrogen XPS signal are in apparent contradiction with those proposed by Brow et al.⁵⁶ Indeed, it has been reported by Hendrickson et al.⁵² that the binding energies of amino groups ($-\text{NH}_2$) vary between 399 and 400 eV. These values are much more lower than those proposed by Brow (Table 2). The N_{1s} signal due to ammonia has been ascribed by Wagner⁵⁸ at a binding energy between 398.7 and 399.7 eV. These results are confirmed by those obtained when ammonia or ethylenediamine is adsorbed on iron surfaces (399.8 or 399.4 eV),⁵⁹ and the data found in the literature for ammonium ions are in agreement with the 400.3–403 eV range.⁵⁸

From all these observations, some conclusions can be made about the nitrogen species included in ZrPON solids. Indeed, XPS analysis, performed on zirconophosphate oxynitrides, shows the presence of two nitrogen chemical forms (three for the less nitrated sample) (Figure 1). In comparison with results obtained for other metallic nitrides (Table 2), it seems clear that the first and less energetic peak around 397 eV is representative of nitride anions N^{3-} . The lower binding energies observed for these species compared to N_{1s} XPS spectra of PON solids^{39,54,55} are consistent with the lower electronegativity of zirconium compared to phosphorus. However, the energy value of 397.7 eV is characteristic of both oxygen and nitrogen environment in PON glasses, and the binding energy decrease observed in Figure 2 is explained by N/O substitution: the lower

value of 397.1 eV could be related to the results obtained for $\text{P}_3\text{N}_5\text{H}_x$ phosphorus nitrides.⁵³ In the case of ZrPON catalysts, no definitive conclusions can be made concerning the coordination level of nitride species, unlike for the metaphosphate glasses, but it can be noted that the width of the band (2.0 eV) allows to suppose the presence of more than one species: in addition to $>\text{N}-$ and $=\text{N}-$ already mentioned, nitrogen can be bonded to the zirconium atoms and/or to the phosphorus atoms, as large bonding possibilities exist.

The second peak located at 399.2 eV can be much debated. It has been chosen to assign it to NH_x species which have been quantified by the Kjeldahl chemical determination. Indeed, the surface atomic concentration of these species reaches the value of 0.4% when expressed in weight concentration, value very close to the N_k chemical determination described in Table 1.

The various hydrogenated nitrogen molecules (NH_3 adsorbed on acid sites, $\text{Me}-\text{NH}_2$ or $\text{Me}-\text{NH}-\text{Me}$) cannot be distinguished from XPS spectra. Nevertheless, DRIFT spectra of ZrPON oxynitrides (Figures 4 and 6) show the presence of NH_3 , $\text{Me}-\text{NH}_2$ and NH_4^+ as an evidence of the presence of such species at the surface. It can be underlined that the thermal treatment (120 °C under 10^{-6} Torr vacuum) of the samples in the XPS preparation chamber theoretically induces the desorption of molecules as NH_3 from Lewis acid sites or NH_4^+ resulting in NH_3 adsorption on Brönsted acid centers. These two types of acid sites on ZrPON surface have been already described in a previous paper.²⁸ So it can be assumed that these two molecules (NH_3 and NH_4^+) are excluded from N_{1s} XPS spectra of ZrPON although they are present on the "fresh" samples: only amino $-\text{NH}_2$ and imido $-\text{NH}-$ groups would contribute to the 399.2 eV component. Nevertheless, the third peak at 400.4 eV observed for the less nitrated sample (1.8 wt % N) could be attributed to ammonium NH_4^+ ions⁵⁸ (Table 2) adsorbed on stronger Brönsted acid sites. Actually, this sample is the most acidic of the series, as it has been already shown that the total acidity (strength and number) of the oxynitrides measured by ammonia chemisorption decreases as well as the number of Lewis acid sites studied by FTIR with pyridine adsorption when nitrogen content increases in the bulk composition.²⁸ The DRIFT spectra also show that the concentration of the ammonium ion (area of the band at 1450 cm^{-1}) is much more important on this sample (1.8wt % N) compared to the other oxynitride samples. Even after heating at 400 °C a weak shoulder is still observed (Figure 4) while this characteristic band has almost completely disappeared at 100 °C on the other less acidic ZrPON (Figure 6).

• *Hypothesis on the Nitridation Mechanism of Amorphous Zirconium Phosphate Powder.* At very low N content, the nitride species content is quite negligible in the oxynitrides samples compared with the NH_2/NH concentration (Figure 3). When total nitrogen content in the bulk is equal to 1.8 wt %, only 25% of the total surface nitrogen atoms have really substituted the oxygen atoms of the zirconophosphate network to produce oxynitride species.

From these observations, a three-stage mechanism, already proposed for the nitridation of silica powder,^{62,63,64} describing the nitridation process of zirconium

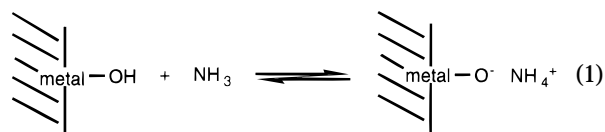
(56) Brow, R. K.; Peng, Y. B.; Day, D. E. *J. Non-Cryst. Solids* **1990**, 126, 231.

(57) Ermdieff, A.; Bernard, P.; Marthon, S.; daCosta, J. C. *J. Appl. Phys.* **1986**, 60, 3162.

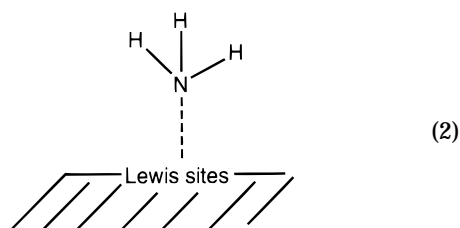
(58) Wagner, C. D.; Riggs, W. M.; Davis, L. E.; Moulder, J. F. *Handbook of X-ray Photoelectron Spectroscopy*; Perkin-Elmer Corporation: Eden Prairie, MN, 1979.

(59) Honda, F.; Hirokawa, K., *J. Electron Spectrosc. Relat. Phenom.* **1977**, 12, 313.

phosphate could be suggested. It is thus assumed that during the nitridation process the flowing ammonia molecules first react with the surface before they substitute the bulk oxygen atoms. Indeed, it has been already shown that the ammonia could react either with the chain terminating metal–OH groups (Brønsted acid sites) to form metal–O–NH₄⁺ ionic bonds

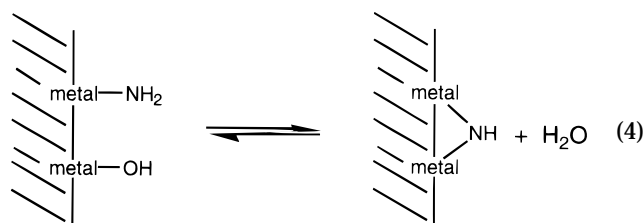
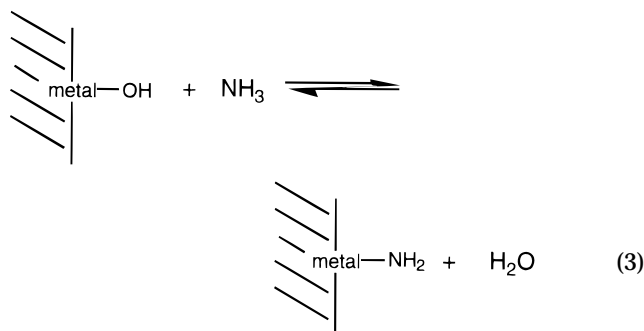


or with Lewis acid sites. In this case, the nitrogen is present on the surface in an adsorbed state:



It is difficult to be sure of the presence of adsorbed ammonia as the characteristic band at 1640 cm⁻¹ in DRIFT spectra is the result of both adsorbed H₂O and NH₃. Nevertheless some NH₃ TPD analyses performed on ZrPON samples have shown that it is possible to adsorb ammonia after degassing the surface by heating treatment under He flow.²⁷ The temperature at which the maximum ammonia desorption occurs is 250 °C. Thus, ammonia may be adsorbed on the ZrPON surface at room temperature.

In a second step, the flowing ammonia will substitute the terminal hydroxyls to form metal amino groups with concurrent release of water molecules and, if the amine and hydroxyl groups react further, a bridging imide is produced with the release of an additional water molecule:



Further condensation of the imide with another metal hydroxyl would give the metal nitride with production

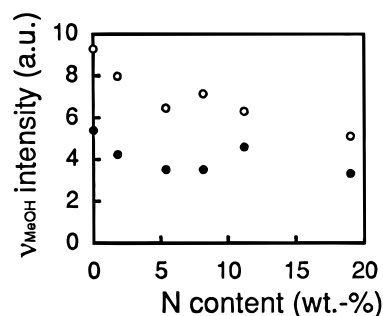
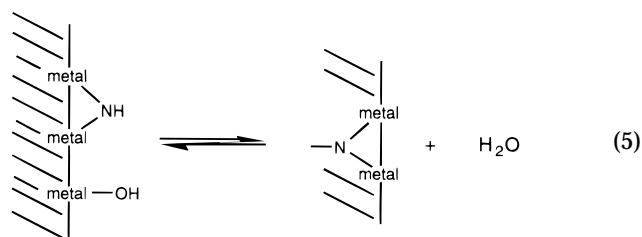


Figure 7. Evolution of the concentration of metal–OH groups detected by DRIFT spectroscopy in zirconium phosphate oxynitride structure after 1 h degassing at 300 °C under N₂ flow: (●) Zr–OH and (○) P–OH.

of an additional water molecule:



Finally, nitridation of the solid network occurs as the nitrogen incorporation in the bulk phase is ensured by diffusion process, as suggested by Bickmore et al.⁶⁴ Thus, even though nitridation is a surface event, the bulk phase can greatly affect the rate and extent of nitrogen incorporation. In the bulk phase, diffusion rates are generally much greater for amorphous materials than for their crystalline counterparts. The mechanism proposed then agrees with previous experimental features obtained at much higher temperatures on crystalline solids. Moreover, precursors with high specific surface area will maximize reaction area.

Figure 3 shows that the XPS concentration of nitride N³⁻ anions increases linearly with the bulk N content. These species become the main nitrogen form when the bulk nitrogen concentration exceeds 5 wt %. The concentration of the surface NH₂/NH species does not change any more when total nitrogen content increases up to 19 wt %, reaching a limiting value close to 4 at. %. Zirconium phosphate oxynitrides, as well as the phosphate precursor, are moisture-sensitive and they adsorb up to 10 wt % water. Therefore, the continuous hydrolysis of the surface could maintain the amine and imide concentration constant once reaction equilibrium of eqs 3 and 4 has been reached. The presence of hydroxyls linked either to zirconium or to phosphorus atoms has been detected by infrared on zirconium phosphate precursor. Their number sharply decreases when the nitrogen concentration increases from 0 to 5.4 wt % (Figure 7) while a weaker evolution is observed for N contents greater than 8 wt %. This observation

(60) Gouin, X.; Grange, P.; Bois, L.; L'Haridon, P.; Laurent, Y. *J. Alloys Compd.* **1995**, 224, 22.

(61) Kang, E. T.; Day, D. E. *J. Non-Cryst. Solids* **1990**, 126, 141.

(62) Mulfinger, O. *J. Am. Ceram. Soc.* **1966**, 49, 462.

(63) Brinker, C. J.; Haaland, D. M. *J. Am. Ceram. Soc.* **1983**, 66, 758.

(64) Bickmore, C. R.; Laine, R. M. *J. Am. Ceram. Soc.* **1996**, 79, 2865.

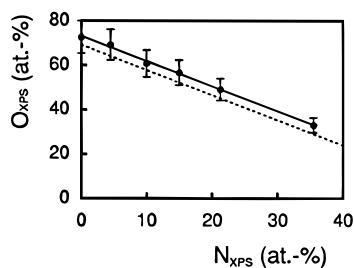


Figure 8. Evolution of XPS oxygen concentration as a function of surface nitrogen content. For comparison, the theoretical O/N bulk relation, established thanks to N_T chemical determination and considering a 3 O/2 N exchange during the nitridation, has been also plotted (dotted line).

reinforce the hypothesis proposed above: an OH/NH_x exchange equilibrium is established when nitrogen content reaches a value greater than 5.4 wt %. However, it must be kept in mind that acid–base reactions at the oxynitride surface also contribute to the decrease of hydroxyl groups concentration.

The surface-hydrolyzed layer has been also observed by XPS spectroscopy since the surface oxygen concentration of the precursor is higher than the bulk theoretical value (Figure 8). This difference is kept constant for all nitrogen contents. However, it must be underlined that the nitridation process occurs simultaneously at the surface and in the bulk solid. Indeed, Figure 8 shows that the evolution of the O–N relation curve at the ZrPON surface is exactly parallel to the theoretical line expected when three oxygen atoms are exchanged in the bulk solid by two nitrogen atoms during the nitridation process.

It can be noted that it seems impossible to totally exchange the oxygen atoms of the bulk oxide during the nitridation step to obtain the Zr_{0.9}PN_{2.9} compound. After 3 days of nitridation at 790 °C, 24% of the starting oxygen atoms still remain in the structure, and the more nitrated sample that has been synthesized has a composition of Zr_{0.9}PO_{1.0}N_{2.2}.^{29,30} The total substitution of oxygen for nitrogen atoms is frequently reported in the synthesis of ceramic powders as AlN or ZrN but these solids are prepared at higher temperatures (> 1200 °C). The soft conditions of ZrPON preparation do not supply sufficient activation energy for the overall oxygen exchange.

The oxygen for nitrogen substitution also induces some structural changes in the environment of both zirconium and phosphorus atoms. Indeed, the binding energy of both cations decreases with increasing nitrogen content ($\Delta E_V = -1.5$ when the N content increases from 0 to 19 wt %). The decrease of the binding energy may be explained by the replacement of oxygen by less electronegative nitrogen inducing a reduction of the average ionic charge of the cations. This indicates then that both new Zr–N and P–N bonds are created at the ZrPON surface whereas some Zr–O and P–O bonds disappear and that the hypothesis of preferential nitridation of one cations may be ruled out. The formation of these new bondings is also proved by the DRIFT spectroscopy. The characteristic P–O stretching vibration around 1260 cm⁻¹ progressively shifts toward a lower wavenumber when nitrogen concentration increases in ZrPON (Figure 6). In addition to its displacement, the band also broadens indicating that nitrogen

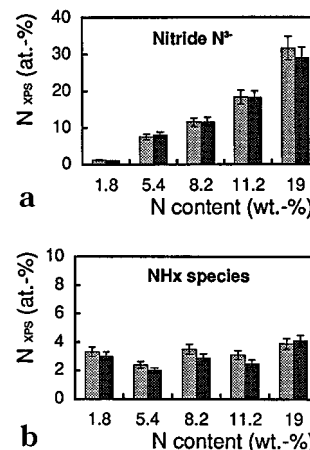


Figure 9. Comparison of the XPS atomic concentration evolution of (a) N³⁻ anions and (b) NH_x species of just nitrated (gray) and 2 years aged samples (black).

atoms are introduced in the phosphorus coordination sphere since absorptions due to P–O and P–N bonds are close to each other.⁶⁵

3.2. Stability of Nitrogenous Species. • *Stability in Air during Storage.* To study the stability of the nitrogenous species, total and surface nitrogen chemical determinations have been reevaluated after a 2 year storage in air of the solid (Table 1). As can be seen from this table, the air exposure of ZrPON catalysts does not induce major modifications of their nitrogen content as very weak differences are observed between the two values, except for the more nitrated ZrPON5 sample. Indeed, the total and the surface nitrogen content of this solid decrease sharper than in other zirconium oxynitrides. The difference could be explained by the departure of physisorbed ammonia present on fresh sample. To support these results, some XPS measurements have also been reproduced. Figure 9 shows a very weak variation of both nitride anions and NH_x species concentration between both experiments. Thus, the difference of nitrogen content in the more nitrated sample, underlined by chemical quantification, is no longer detected by XPS determination. However, it cannot be excluded that weakly adsorbed species are easily eliminated under high vacuum conditions. Diffusion of bulk N³⁻ species, at room temperature, is hardly explained. However, it has to be noted that, under hydrolysis–heat treatment cycles, diffusion AIPON solids bulk N³⁻ species, at room temperature, is hardly explained. However, it has to be noted that, under hydrolysis–heat treatment cycles, AIPON solids bulk N³⁻ concentration decreases while surface nitrogenous species concentrations are not changed.⁶⁶

• *Thermal Stability. a. Experimental Results.* Figure 10 shows a TPD–MS spectrum of ZrPON4 (11.2 wt % N) heated under pure He flow. Several ions are identified: H₂O ($m/e = 18$), NH₃ ($m/e = 17$) and N₂ ($m/e = 28$) have been detected. It is assumed that no atmospheric CO₂ nor N₂O molecules are desorbed from ZrPON solids as no $m/e = 44$ have been found in the total mass spectrum. The $m/e = 18$ curve shows a peak located at

(65) Benitez, J. J.; Diaz, A.; Laurent, Y.; Grange, P.; Odriozola, J. *A. Z. Phys. Chem.* **1997**, *202*, 21.

(66) Centeno, M. A.; Debois, M.; Grange, P. *J. Phys. Chem.* **1998**, *102*, 6832.

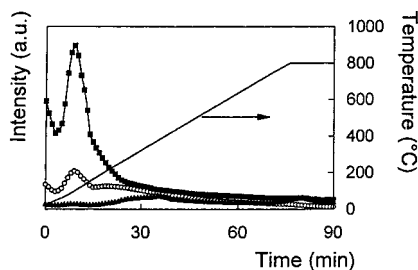


Figure 10. TPD-MS analysis of gas reaction products of ZrPON4 (11.2 wt %) heated to 800 °C under He flow: (○) $m/e = 17$ (NH_3 and H_2O), (■) $m/e = 18$ (H_2O), and (▲) $m/e = 28$ (N_2).

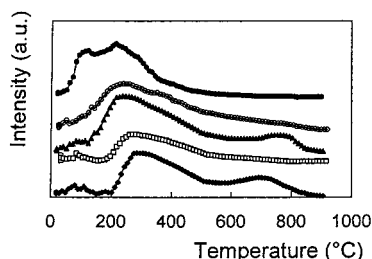


Figure 11. Evolution of ammonia desorption from ZrPON surface heated to 800 °C under He flow and followed by mass spectroscopy: (◆) 1.8, (□) 5.4, (▲) 8.2, (○) 11.2, and (●) 19 wt % N.

120 °C that corresponds to the maximum water elimination. This temperature does not vary with the nitrogen content. The evolution of desorbed ammonia is evaluated by the profile of $m/e = 17$ (ammonia + water) from which the participation of $m/e = 18$ (only water) have been subtracted as explained in the Experimental Section. The elimination of ammonia takes place in three steps (Figure 11). The first one occurs at low temperature (120 °C) and corresponds to weakly physisorbed ammonia or ammonia adsorbed on Lewis and Brönsted acid sites. The second ammonia desorption is the most important and appears between 200 and 500 °C. The maximum of this peak decreases from 280 to 220 °C when nitrogen content increases from 1.8 to 19 wt %. These two first stages have been already observed and described for AlPON oxynitrides.⁶⁵ A third departure of nitrogen as ammonia is observed at high temperature (750 °C) for some ZrPON samples (ZrPON1 and ZrPON3). The concentration of all these desorbed ammonia molecules have been established by titration measurement and the values obtained are very low: they are comprised between $0.06 < \text{N wt \%} < 0.16$.

The ZrPON samples pretreated at 800 °C under He flow have been then analyzed by XPS spectroscopy. The high-temperature treatment does not seem to influence in a large extent the surface nitrogen content as weak modifications of nitrogen surface concentration are observed before and after the heating (Figure 12). Indeed no major variations are observed between fresh and treated samples except for ZrPON1 for which the NH_x concentration is reduced by half after heating at 800 °C.

These observations prove that ZrPON oxynitrides are not sensitive to hydrolysis since no special care was taken in the storage between the pretreatment and the XPS analysis.

The thermal evolution of nitrogen species has also been studied by DRIFT spectroscopy (Figure 4). When

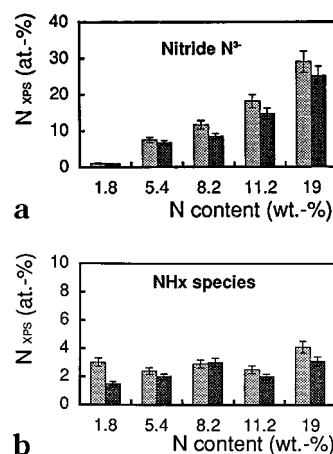


Figure 12. Comparison of the XPS concentration evolution of (a) N^{3-} anions and (b) NH_x species: (gray) fresh samples (without any pretreatment); (black) the same samples pretreated 1 h at 800 °C under He flow.

ZrPON samples are heated until 100 °C under nitrogen flow, the NH_4^+ vibrations at 1420 cm^{-1} have nearly completely disappeared except for the less nitrated sample for which a temperature of 400 °C has to be reached for the complete desorption of ammonium cations. The concentration of adsorbed ammonia and water (vibration at 1640 cm^{-1}) decreases sharply under heating to result in a weak shoulder superimposed to the main signal at 300 °C. Further heating leads to the elimination of this last peak while a temperature of 400 °C has to be reached to observe a decrease of Me-NH_2 concentrations. In the $3000\text{--}4000 \text{ cm}^{-1}$ spectral area, progressive heating leads to a better resolute spectrum: two fine peaks appear after water desorption. They are assigned to the vibrational mode of hydroxyl groups bonded to phosphorus ($\nu_{\text{POH}} = 3660 \text{ cm}^{-1}$) and to zirconium ($\nu_{\text{ZrOH}} = 3740 \text{ cm}^{-1}$) atoms. The large band around 3240 cm^{-1} (NH_x stretching vibrations) also becomes sharper and well defined after the heating.

b. Discussion. Thanks to the combination of DRIFT spectra and mass spectroscopy results, Benitez et al.⁶⁵ have studied the thermal stability of aluminophosphate oxynitrides AlPON. They proposed the elimination of nitrogen as ammonia in two stages: the first at low temperature (100–130 °C) which corresponds to ammonia adsorbed on Lewis and Brönsted acid sites and the second at 330 °C when terminal P-NH_2 are attacked by gaseous water coming from hydroxyl condensations. As related by these authors, interesting information about changes produced by heating may be obtained by subtraction of two DRIFT spectra corresponding to a temperature interval in which a change is expected.

On the basis of the method followed by Benitez et al., the thermal evolution study of ZrPON samples described in this paper has been performed. Each plot in Figure 13 shows the result of the subtraction between the spectra obtained at two consecutive temperatures. The difference spectra of ZrPON1 (1.8 wt % N), ZrPON3 (8.2 wt % N), and ZrPON 5 (19 wt % N) are plotted. The positive peaks are indicative of generated species and negative bands are due to eliminated ones when the lower temperature is used as background. As for AlPON solids, the nitrogenous species stability in ZrPON powders may be explained by different steps

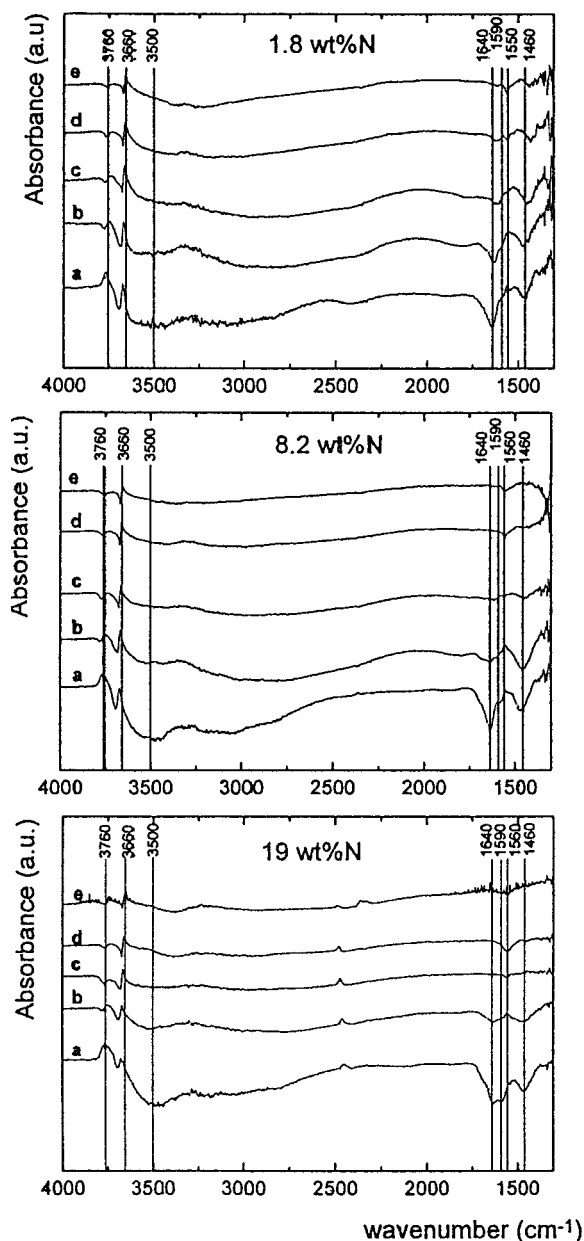


Figure 13. DRIFT difference spectra of fresh ZrPON samples with various N content: (a) 100 °C to room temperature; (b) 200–100 °C; (c) 300–200 °C; (d) 400–300 °C; (e) 500–400 °C.

according to the temperature range considered. However, metal cations (aluminum or zirconium) can be seen to influence the thermal behavior of the oxynitride powders since some differences between ALPON and ZrPON solids may be pointed out. For more clarity in further discussion, the various temperature ranges will be successively studied.

•First when zirconophosphate oxynitrides are heated from room temperature until 200 °C under inert atmosphere, the desorption of physically adsorbed water occurs (Figure 10). This observation is made for all samples of the series and is confirmed by the DRIFT difference spectra as indicated by the negative band at 1640 cm^{-1} and around 3500 cm^{-1} (spectra a and b in Figure 13). In the same temperature range, ammonium cations, resulting from ammonia adsorption on Brønsted acid centers, are also removed from the surface (negative band at 1460 cm^{-1}). It can be underlined that

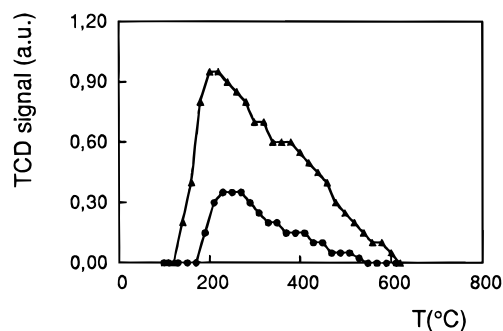


Figure 14. Ammonia TPD analysis of the precursor (ZrPO) (▲) and the zirconophosphate oxynitride (5 wt %) (●) after 1 h pretreatment at 800 °C under He flow (from reference 27).

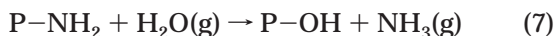
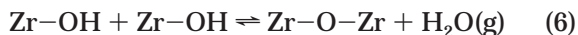
complete desorption of NH_4^+ is realized at 200 °C on ZrPON3 and ZrPON5 (no more change at 1460 cm^{-1} on spectrum c in Figure 13) but 400 °C has to be reached for total elimination of ammonium cations on the less nitrated and more acidic sample. The Brønsted acid sites have been associated with surface hydroxyl groups identified by DRIFT spectroscopy. It is then quite logical to observe concurrently the appearance of new hydroxyl groups as proved by two positive peaks in the 3500–4000 cm^{-1} range. The restoration of hydroxyls is due not only to NH_4^+ desorption but also to the removal of water under heating. Higher temperatures are required for ammonia elimination from Lewis acid centers, and as seen in Figure 11, the ammonia desorption profiles are similar whatever the N content. Nevertheless the curve characteristic of NH_3 desorption from ZrPON5 surface (19 wt % N) shows an additional maximum around 120 °C. This first stage is attributed to the elimination of weakly physisorbed ammonia as suggested by the negative peak at 1590 cm^{-1} juxtaposed to the negative signal due to water departure at 1640 cm^{-1} (spectra a and b in Figure 13). This signal is also observed for ZrPON3 (8.2 wt % N) and for ZrPON1 (1.8 wt % N), but its intensity is much more reduced compared to ZrPON5. Thus the concentration of physisorbed ammonia seems to be more important on more nitrated samples. It can be noted that XPS spectroscopy does not allow the detection of such species as pretreatment under vacuum in the preparation chamber would probably involve their total removal before the analysis step.

•When the temperature is raised to 400 °C, a second ammonia desorption step is observed, indicative of the presence of Lewis acid sites (Figure 11). These sites are most probably due to the presence of coordinatively unsaturated and exposed Zr^{4+} cations. Figure 11 may be compared to the profile of ammonia desorption curves during NH_3 -TPD experiments, performed in order to characterize the ZrPON acidity (Figure 14).²⁷ In these experiments, the catalyst surface is first degassed for 1 h at 800 °C under He flow, and ammonia is then adsorbed at 150 °C for 15 min before being quantified by desorption under He flow up to 800 °C. In both cases, the desorption occurs between 150 and 550 °C with the maximum temperature located between 200 and 300 °C, and the desorption signal is asymmetric with a large tail at high temperature indicative of acid strength heterogeneity. The maximum of ammonia desorption during pretreatment shifts toward low temperature when the nitrogen content increases in ZrPON. This

result was expected as it has been already shown that the acid strength decreases when nitrogen atoms are incorporated in zirconophosphate structure.²⁸ Figure 13 (curves a and b) shows that ammonia (1640 cm^{-1}) is still desorbed from ZrPON1 (1.8 wt % N) and ZrPON3 (8.2 wt % N) in the $300\text{--}400\text{ }^{\circ}\text{C}$ range (water contribution being completely neglected in this temperature range) while the ammonia concentration does not longer change above $200\text{ }^{\circ}\text{C}$ for ZrPON5 (19 wt % N).

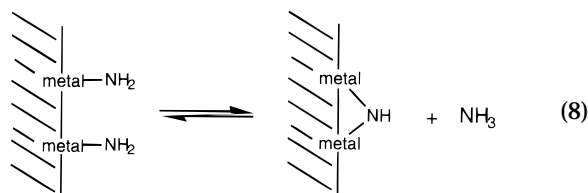
•Above $400\text{ }^{\circ}\text{C}$, ammonia characteristic infrared vibrations have completely disappeared whatever the N content; this observation is inconsistent with the mass spectroscopy result as total desorption of NH_3 does not end before $500\text{ }^{\circ}\text{C}$ (Figure 11). An explanation may be put forward by comparison with observations made by Benitez et al. on ALPON solids.⁶⁵ After complete ammonia desorption from Lewis and Brönsted acid sites, these authors proposed the elimination of amino ($-\text{NH}_2$) groups linked to phosphorus atoms due to gaseous water coming from hydroxyls condensation, $\text{P}-\text{NH}_2 + \text{H}_2\text{O} \leftrightarrow \text{P}-\text{OH} + \text{NH}_3(\text{g})$. Their hypothesis is emphasized by the appearance of new P-OH species.

Figure 13 shows the disappearance of amine groups above $200\text{ }^{\circ}\text{C}$ for ZrPON5 (19 wt % N) and above $300\text{ }^{\circ}\text{C}$ for ZrPON1 (1.8 wt % N) and ZrPON3 (8.2 wt % N) (negative band at 1550 cm^{-1}). In the case of zirconium phosphate oxynitrides, it has been chosen to attribute the infrared band at 1550 cm^{-1} to N-H vibrations in metal-NH₂ without distinction between phosphorus or zirconium atoms. Indeed, Lednor et al.⁴⁶ as well as Liu et al.⁴⁷ mentioned it as the characteristic vibration frequency of the N-H bond in Si-NH₂ and Al-NH₂ groups, respectively. Therefore, this vibration does not seem to be much influenced by the nature of the metal bonded to nitrogen atoms. At the same temperature, in the $3500\text{--}4000\text{ cm}^{-1}$ energy range, the concentration of Zr(OH) species decreases while the concentration of P(OH) groups continues to increase (negative band at 3760 cm^{-1} and positive band at 3660 cm^{-1}). If the scheme proposed by Benitez et al. for the explanation of amine disappearance is taken into account, this last result may be representative of Zr-OH condensation while water produced induces the appearance of new P-OH groups:



The gaseous ammonia liberated would correspond to the TPD signal still observed between 400 and $500\text{ }^{\circ}\text{C}$ for ZrPON1, ZrPON2, ZrPON3, and ZrPON4 in the Figure 11. Above $400\text{ }^{\circ}\text{C}$, the low TPD signal of ZrPON5 is representative of a very weak NH_3 desorption. The hydrolysis of amine terminal groups (eq 7) is consequently completed. This conclusion is confirmed by DRIFT spectroscopy: no more change is observed for ZrPON5 (19 wt %) on spectra e in Figure 13. It must be underlined that eq 7 does not involve all NH_2 groups as the 1550 cm^{-1} typical vibration is still observable in Figure 4 at temperatures up to $700\text{ }^{\circ}\text{C}$ for ZrPON5. In the same way, some Zr(OH) groups remain at the surface of ZrPON solids because of the presence of an infrared band at 3760 cm^{-1} (Figure 4).

•Around $700\text{ }^{\circ}\text{C}$, final ammonia desorption occurs at the surface of two samples (ZrPON1 1.8 wt % and ZrPON3 8.2wt %) (Figure 11). This observation could perhaps be explained by amine condensation resulting in the formation of metal imido groups with release of ammonia molecule:



However, it must be kept in mind that the concentrations measured by mass spectroscopy are very low. Indeed, the chemical quantity determinations of nitrogen desorbed upon heating give values lower than 0.2 wt %. This result is confirmed by XPS measurement: there is no significative change in the surface nitrogen concentration between the fresh and the pretreated samples except for NH_x species of the less nitrated sample (Figure 12). Total nitrogen determinations have been also realized for ZrPON5 heated to $800\text{ }^{\circ}\text{C}$, and a value of 16.6 wt % has been found. This value must be compared to the 17.2 wt % obtained for a fresh sample aged for 2 years. The 3.5% relative error may be attributable to the experimental uncertainty of the method. ZrPON oxynitrides are then thermally stable compounds, and this characteristic is very important for their further application in catalysis.

4. Conclusion

Two types of nitrogen species have been identified at the surface and in the bulk zirconium phosphate oxynitride powders. The first one consists of the nitride N^{3-} anions introduced in the phosphate network during the nitridation in exchange to oxygen atoms; three oxygens being replaced by two nitrogens in order to maintain the charge balance of the solids. The second nitrogenous type species regroups various surface NH_x molecules with $1 \leq x \leq 4$. These hydrogenated compounds are formed when the nitriding agent (NH_3) reacts with the ZrPON surface. Indeed, both NH_4^+ and adsorbed NH_3 have been identified as the result of an acid-base reaction between flowing ammonia and Brönsted or Lewis acid centers, respectively. On the other hand, the presence of amino ($-\text{NH}_2$) and imido ($-\text{NH}-$) groups is explained by surface hydroxyl substitution during the activation process leading to water departure. The evolution of the various nitrogenous species concentration when total nitrogen increases in the catalyst framework allows us to propose a mechanism describing the nitridation of ZrPON powder.

The ZrPON catalysts are stable in atmospheric conditions and no special care must be taken concerning their storage. Their thermal stability has been also established by combination of TPD-MS and DRIFTS results, and it appears that nitrogen is removed from the ZrPON powder by a three-step desorption process depending on the temperature range considered. First, at low temperature ($<200\text{ }^{\circ}\text{C}$), weakly physisorbed ammonia as well as ammonia adsorbed on Brönsted acid sites is

desorbed from the surface. Second, in the 200–400 °C range, ammonia liberated the Lewis acid sites. At higher temperatures, terminal amine groups are attacked by gaseous water coming from hydroxyl condensation, which results in the appearance of new hydroxyls bonded to phosphorus atoms. Nevertheless, whatever the nitrogen content present in the solids, the desorbed ammonia concentrations are very low (<0.2 wt %). ZrPON oxynitrides are then characterized by a high thermal stability which is of crucial importance for their further use in catalysis.

Acknowledgment. N.F. thanks the “Fonds pour la Formation à la Recherche dans l’Industrie et dans l’Agriculture”, F.R.I.A., for a grant. M.-A.C. thanks the European Union for a “Training and Mobility of Researchers” (TMR) postdoctoral grant. We acknowledge the financial support of the “Région Wallonne” and the “Fond National de la Recherche Scientifique”, Belgium.

CM980732E